Exploring the explosive ablation regime of metals in nanosecond micromachining

Jennifer M. Fishburn, Richard P. Mildren, Daniel Kapitan [b], Michael J. Withford, Daniel J.W. Brown & James A. Piper.

Centre for Lasers & Applications
Division of Information and Communication Sciences
Macquarie University, NSW 2109, Australia
Ph: 61 2 9850 8964
Fax: 61 2 9850 8983
Email: jenn@ics.mq.edu.au

[b] University of Oxford
Department of Atomic and Laser Physics
Clarendon Laboratory
Oxford OX1 3PU UK

ABSTRACT

We present results of single shot ablation experiments for a variety of metal samples (In, Al, Cu, Mo, W, Ti) using visible, nanosecond lasers at fluences up to ~10^4 J cm^{-2}. At low fluences, usually less than 10^2 J cm^{-2}, small amounts of material were removed and removal was approximately uniform across the ablation crater. As the fluence increased above ~ 10^2 J cm^{-2}, substantially more material was removed and a conical pit developed in the centre of the ablation crater. The appearance of these conical pits is consistent with material removal by phase explosion mechanisms. In this paper, this ablation phenomenon will be investigated by presenting the crater morphology as a function of fluence. Consequences for micromachining with visible, high repetition rate, nanosecond lasers will be discussed.

Keywords: phase explosion / nanosecond machining / laser machining

1. INTRODUCTION

Direct write laser percussion drilling or milling is rapidly becoming the method of choice for manufacturing microscopic structures (10-300μm) in the aeronautic, biomedical, electronic, and scientific industries. Achievable structural resolution (<1μm) and flexibility far surpasses conventional mechanical machining methods. In addition, the fast processing rates available to direct write laser processes in materials such as metals, polymers, and ceramics compare favourably with the processing rates for alternative micron-scale processes such as EDM and lithography.

Introduction of this direct write laser micromachining technique into an industrial setting requires an in depth knowledge of the processing times and limits of resolution. Therefore it is important to investigate and characterise the physical ablation mechanisms at play in pulsed laser ablation. Such investigations [1-4] have shown that pulsed laser ablation occurs via several physical regimes and is highly dependent on wavelength, pulse length, pulse energy, fluence of the incident beam and on the properties of the material to be ablated. Ablation of metals in the nanosecond regime has been shown to be predominantly thermal in nature [4]. Briefly, in order of increasing fluence, the regimes understood to be influential in visible nanosecond drilling are;

a) Evaporation –direct vaporisation of metal from the liquid melt pool.
b) Melt Expulsion- expulsion of liquid metal from a melt pool, by either of the following mechanisms;
   (i) Pressure Recoil – the creation of a pressure front into the melt pool expels the melted liquid.
   (ii) Phase explosion – the creation of small vapour nuclei causes the material to be expelled from within the melt pool.

In *High-Power Laser Ablation II*, Claude R. Phipps, Masayuki Niino, Editors,
Proceedings of SPIE Vol. 3885 (2000) • 0277-786X/00/$15.00

Nanosecond drilling at high fluences (>100J cm^{-2}) [5], appears to occur under a liquid material removal or melt expulsion regime. A phenomenon that is being increasingly proposed to explain the high ablation rates observed under these conditions is that of *Phase Explosion.* The liquid metal acting under this regime is heated in a short time scale (<1μs) [6] by high fluence laser radiation and becomes superheated. The excess energy within the system causes the superheated melt pool to experience homogeneous nucleation (spontaneous creation of vapour bubbles within the melt) [7]. If created with a suitably large radius these bubbles increase rapidly in size and give the expelled particles of melt a kinetic energy. This heat to kinetic energy transfer causes large amounts of liquid metal to be removed resulting in enhanced localised material ablation. Indications are strong that this explosive boiling material removal occurs at approximately 0.9 times the critical temperature (T_c) [8] (the temperature above which the sample cannot exist in liquid form under any pressure conditions).

Recently Kapitan et al [9] collated data from several ablation studies with the intention of identifying the different ablation regimes encountered for different fluences and pulse durations. This suggested that the transition between evaporation and melt expulsion material removal for nanosecond laser sources lies in the region 10^2-10^3 J/cm^2. However, Mele et al. [10] determined that a transition occurred at a fluence of only 6-8 J/cm^2 in the ablation of Aluminium samples with a frequency doubled Nd:YAG (pulse length ~6ns). In this case, the transition was identified by an observation of marked increases in the light emitted by the vapour plume as fluence was increased.

Further to these studies, we present experimental data mapping the transition from evaporation to melt expulsion for single shot ablation by visible nanosecond pulses in a number of common and refractory metals. These metals (In, Al, Cu, Ti, Mo & W) have been chosen to represent easily accessible materials that are commonly used in industry, with diverse thermodynamic properties. Wide ranges of fluences (50~10000J/cm^2) were utilised in single pulses to maximise the possibility of inducing an explosive form of melt expulsion. The fluence thresholds found for a phase explosion regime associated with visible nanosecond pulses are consistent with those proposed by Kapitan et al. Our findings are discussed in relation to issues of resolution and drill speed.

2. EXPERIMENTAL DETAIL

1. Laser Source and Ablation Geometry

The laser source used was a pulsed low temperature Copper HyBrID laser [11], producing a maximum average power of 100W of polarised visible output (511 & 578 nm) with a 40ns pulse duration at a repetition rate of 12.3 kHz. Unlike conventional Copper Lasers this source produces a quasi-Gaussian beam profile. The beam was 25mm diameter and was focused onto the substrates using a 200 mm focal length achromat lens (Figure 1). Each metal was oriented in the horizontal plane and attached to a mount that ran down a track at 15° to the vertical. This enabled not only each pulse to fall incident on a new portion of sample, but also for each successive pulse to ablate the sample at a different focal position. A wave

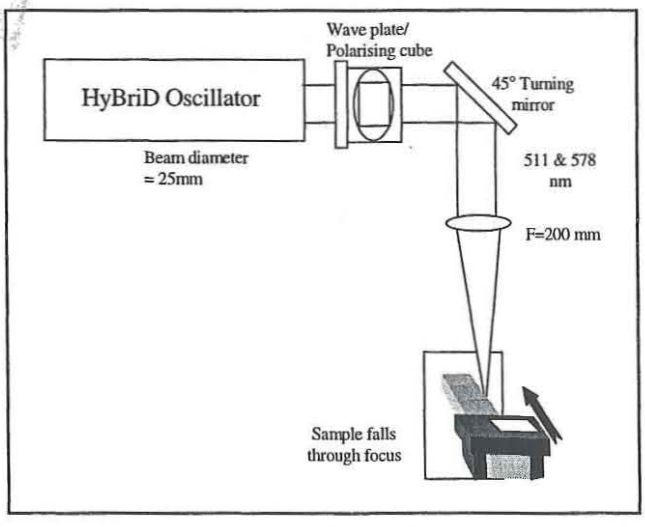

Figure 1: Experimental Layout

plate-polariser cube was used to reduce the energy in each consecutive run through focus, whilst all other pulse characteristics (duration, repetition rate, temporal profile & spot-size) remained equal. We were therefore able to study craters ablated at the same spot size with different incident fluences as well as craters ablated at different spot sizes with similar fluences.

2. Metals Under Review

The samples under study were divided into common (In, Cu, Al) and refractory (Ti, Mo, W) metals (Table 1). They underwent no pre-drilling polishing or chemical preparation with the exception of cleaning with a standard alcohol wipe.

Metal	*Symbol [Unit]*	*Indium (In)*	*Aluminium (Al)*	*Copper (Cu)*	*Titanium (Ti)*	*Molybdenum (Mo)*	*Tungsten (W)*
Melting Point	T_m[K]	429.5	933.3	1357	1943	2896	3695
Boiling Point	T_b[K]	2343	2793	2833	3563	4913	5823
Critical Temp[1]	T_c[K]	4520	5410	5890	7890	10780	13890
Heat of fusion	H_f[J g^{-1}]	63	407	204	322	375	190
Heat of vaporisation	H_v[J g^{-1}]	4470	10777	5125	8937	6145	4480
Density	ρ [g cm^{-3}]	7.29	2.698	8.933	4.508	10.222	19.254
Specific Heat	C_p[J g^{-1} K^{-1}]	0.231	0.88	0.379	0.511	0.246	0.133
Thermal Conductivity	k[J s^{-1} cm^{-1} K^{-1}]	0.84	2.36	4.03	0.22	1.39	1.77
Thermal Diffusivity	κ[cm^2 s^{-1}]	0.499	0.994	1.190	0.096	0.553	0.691

Table 1 : Material Properties [12 &13]

3. Measurement Methods

Crater depths and diameters were measured using differential focussing in an Olympus optical microscope with a micrometer-actuated z-stage. A JEOL JSM-840 Scanning Electron Microscope was used to obtain high resolution images of the craters.

4. Crater Morphology

In general, crater morphology is a useful tool for identifying the ablation regime at a given fluence. At lower fluences there is uniform material removal from the regions of visible surface change of the substrate, melting can be seen but there are no areas of preferential ablation. At higher fluences (typically > 10^2 J cm^{-2}) the creation of small, deep pits (Figure 2) in the centre of the ablated region provides evidence that a transition to an enhanced material removal regime has occurred. In general, the depth of this central pit is much greater than that of the region surrounding it.

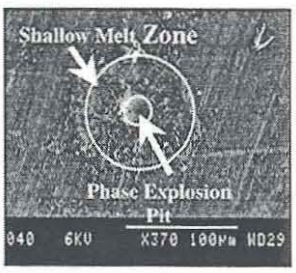

Figure 2: Melt zone and explosion pit

3. RESULTS & DISCUSSION

1. Spot size and Fluence.

Characterisation of dominant material ablation regimes is generally expressed in Fluence (J/cm^2), Irradiance (W/cm^2), or Energy density (J/cm^3). It is imperative have an accurate measurement of fluence (hence spot size) for a given pulse energy or power. Based on experimental measurements of spot-size through the focus of our drill lens, an analysis of the fluence as a function of distance from focus for the optical system implemented in this work is provided in Figure 3. A 200mm focal length lens, 511nm output and a beam diameter of 25mm, gave a minimum spot size of ~8µm (the spot size is defined as the diameter within which perimeter 87% of the energy in confined). Despite being only quasi-Gaussian in nature, the beam's spot size dependence on distance from focus was shown to follow a Gaussian fit applied to the data (ω_0 = 8µm and z_R = 75 µm). The corresponding fluence mapping shown is for a pulse of ~5.4 mJ energy. The maximum fluence, obtained at focus, had a value ~10^4 J cm^{-2}.

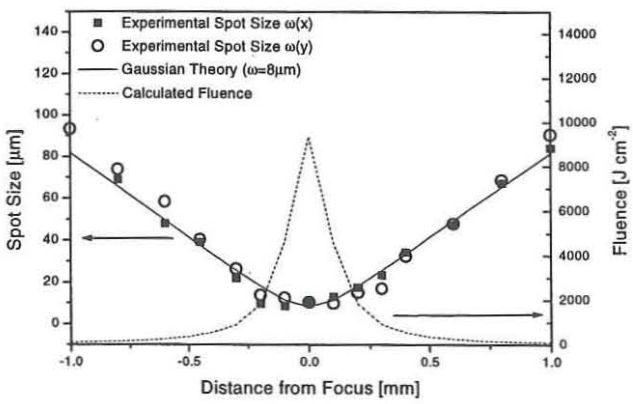

Figure 3: Experimental spot size and calculated fluence

2. Crater Depths

Figures 4 & 5 present data of the ablation depths of both common and refractory metals at two different pulse energies (0.43 mJ & 5.4 mJ). The depths have been represented as a function of the irradiating fluence. The crater depths at both pulse energies in descending order are Indium, Aluminium, Copper, Titanium, Molybdenum and Tungsten. Note that this sequence is exactly that of the (ascending) sequence of melting point and critical temperatures of the metals. It is seen that the refractory metals exhibit crater depths almost an order of magnitude lower than those seen in common metals. Note also that the ablation depths for both common and refractory metals appear to saturate at higher fluences.

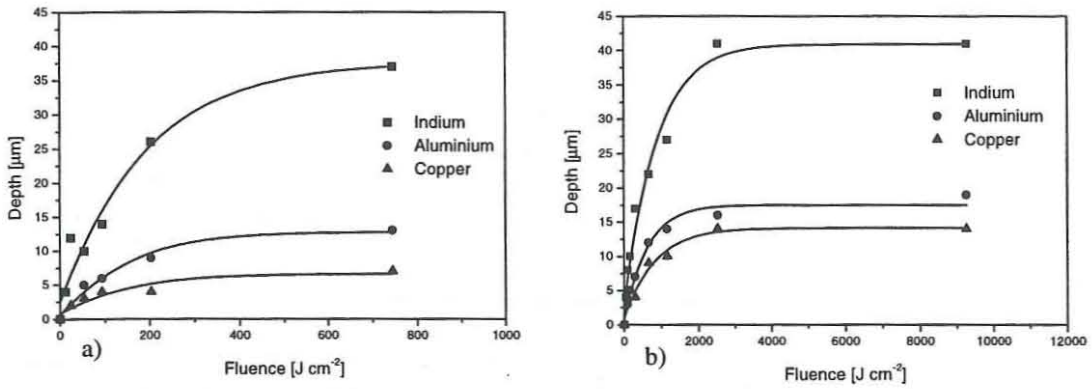

Figure 4: Crater depths in common metals for incident pulse energies of a) 0.43mJ & b) 5.4 mJ

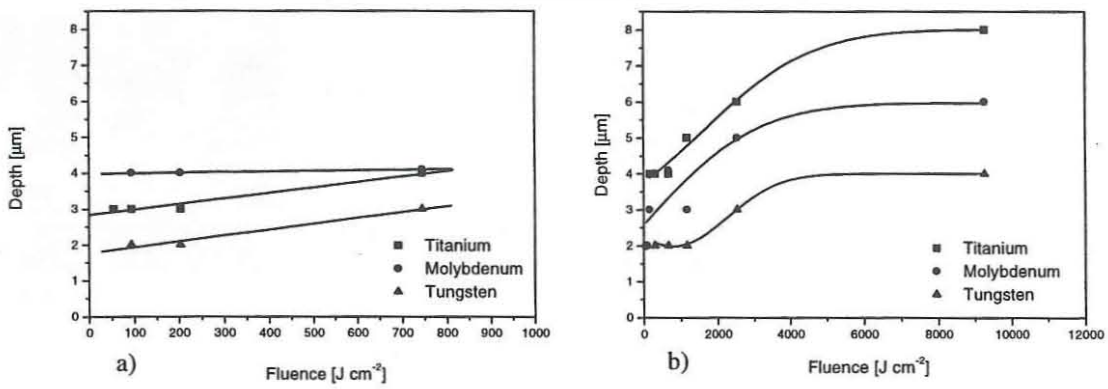

Figure 5: Crater depths in Refractory metals for incident pulse energies of a) 0.43mJ & c) 5.4 mJ.

3. Crater Morphology Analysis

In addition to analysing the depths of the ablation pits created in the metal samples, the crater and central pit diameters were measured to provide information about the effect of fluence on feature resolution. In this case, all samples were ablated at focus to provide a useful comparison between craters with all spatio-temporal parameters remaining the same, a

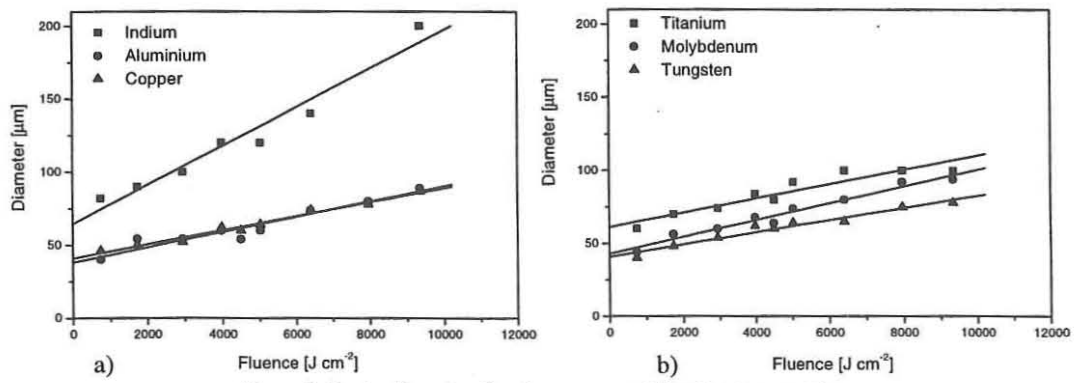

Figure 6: Crater diameters for a) common and b) refractory metals.

fixed spot size with only the incident fluence changing from point to point. Figure 6 shows the total crater diameter, measured as the outer rim of the melt zone (Figure 2). It can be concluded from this data, that all metals experience a reduction in crater diameter with decreasing fluence. The rate of this reduction is highly dependent on the sample properties. Indium manifests the greatest change in crater diameter, followed jointly by Aluminium and Copper and then, with much shallower slopes, follow Titanium, Molybdenum and Tungsten.

The data make it clear that the interplay between thermal diffusion and the ablation characteristics is not elementary. Reviewing these results suggests that although a sample may have a low themal diffusion constant thereby maintaining a higher sample temperature at the point of irradiance, it is the melting temperature that ultimately controlls the overall ablation depths. Also, the change in feature size seems to be associated more strongly with the melting temperature than the thermal diffusivity or the specific heat of the sample.

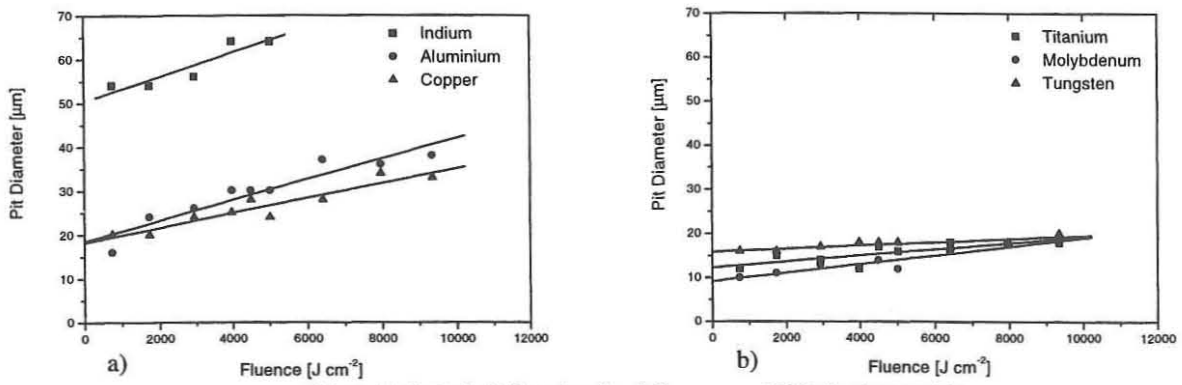

Figure 7: Central pit diameters for a) Common and b) Refractory metals.

Figure 7 presents data on the spatial evolution of the central pit with increasing fluence. Once again the common metals follow a trend related to the temperature properties of the sample. Anomalously, in the case of the refractory metals, Tungsten consistently exhibits a larger central pit radius at lower fluences than either Titanium or Molybdenum despite having a higher melting temperature.

4. Thresholds for Phase Explosion

As a result of obtaining data using a "moving through focus" technique for several different pulse energies, it was possible to identify the onset of a high material removal regime (Phase Explosion) by the earliest signs of a central pit within the crater. A sample of an ablation run in Molybdenum is shown in Figure 8, where the appearance of the characteristic central pit occurs at a fluence of ~ 100 J cm^{-2}. Note that the irradiation spot size decreases from 75µm to 8µm at focus.

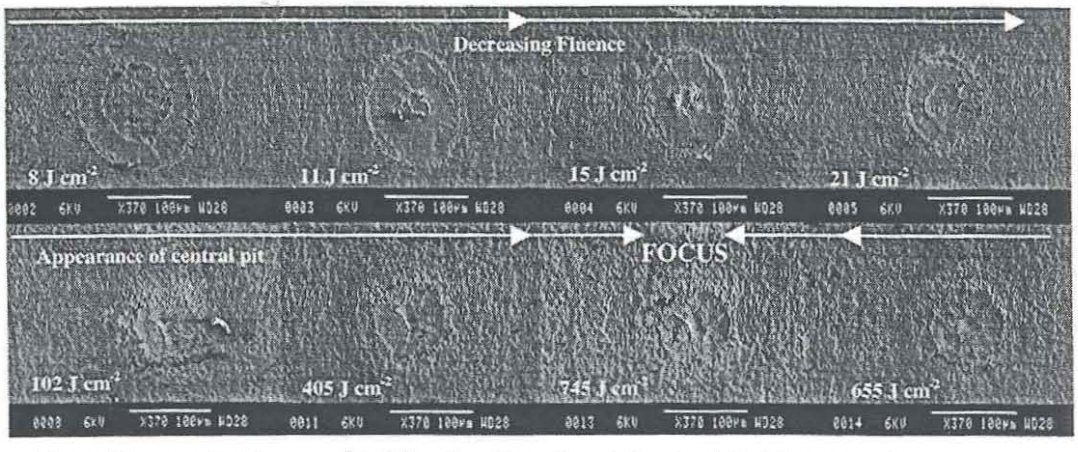

Figure 8: Images of craters created at different posistions thorugh focus in a Molybdenum sample.

In this manner, for different pulse energy ablation runs, the fluence at the initial appearance of the central pit was determined for all samples (both common and refractory metals) and is presented in Figure 9.

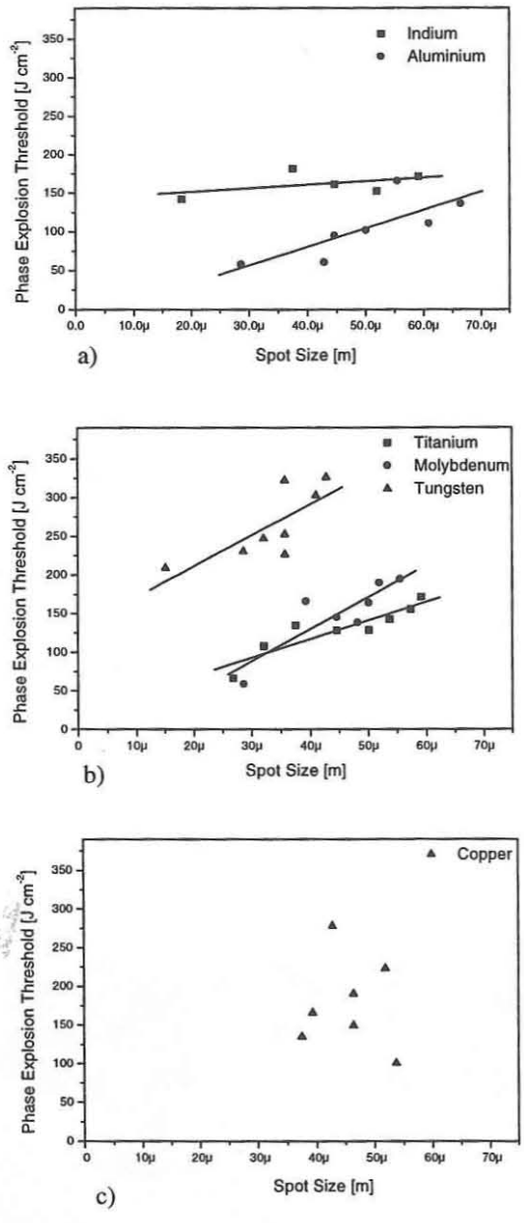

Figure 9 : Phase Explosion Threshold Fluences for a) Indium and Aluminium, b) refractory metals & c) Copper.

Common and refractory metals alike, with the exception of Copper, demonstrate a weak dependence of phase explosion threshold on spot size (increasing with increasing spot size). Interestingly, our results do not evidence a clear correlation between the samples' temperature parameters and the onset of phase explosion. As might be expected, Tungsten exhibits consistently the highest phase explosion threshold (200~325 J cm^{-2}), but it is then followed fairly closely, with no readily discernible order, by the other metals' explosive thresholds (50~ 200 J cm^{-2}). For all materials studied, pits began to appear

in the centre of craters within the region 50~325 J cm^{-2}. This is consistent with the predictions of Kapitan et al. that the shift from an evaporative regime to one of melt expulsion occurs for nanosecond pulses at fluences of approximately 10^2~10^3 J cm^{-2}.

Phase explosion is a phenomenon crucially linked to sample parameters such as melting temperature and critical temperature. It was expected that the threshold fluence for phase explosion in each metal should be fairly constant regardless of the spot size of the incident pulse falling on the sample as long as the fluence remained the same. However, the results indicate that with increasing spot sizes there is an increase in the threshold required for phase explosion.

To determine the importance of the spatial beam profile on phase explosion thresholds, we have calculated the peak fluences in a 1μm radius at the centre of the beam. Data presented in Figure 10, showing peak fluences at phase explosion thresholds as a function of spot size, demonstrate that the thresholds for common and refractory metals remain spot size dependent even when beam profile changes are taken into account. This unexpected result will be the subject of further investigations.

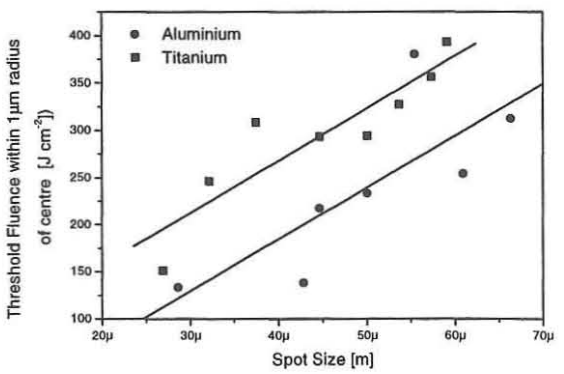

Figure 10: Titanium and Aluminium data presented as fluences over the central 1 micron radius for phase explosion thresholds as a function of spot size.

4. CONCLUSION

Results presented in this work show that at comparable fluences the ablation rates for Indium are approximately 5~6 times and for Copper and Aluminium are a factor of 2~3 higher than those in selected refractory. Crater depths follow the sequence of melting and critical temperatures for each metal; the higher the melting temperature, the lower the crater depth. Phase explosion thresholds were identified in this study by the appearance of a pit in the central region of the ablation crater. It has been shown that in all metals, regardless of thermodynamic properties, these pits begin to appear within the fluence region 50-325 J cm^{-2}. An unexpected and potentially significant outcome is that for some metals the fluence at threshold for phase explosion is lower for small irradiation spot sizes. These results may prove significant for choice of ablation conditions in order to achieve high material removal rates in the phase explosion regime.

5. REFERENCES:

1. J. Jandeleit, A. Horn, R. Weichenhain, E. W. Kreutz and R. Poprawe, " Fundamental investigations of micromachining by nano- and picosecond laser radiation," *Applied Surface Science* **127-129**, pp 885-891, 1998.
2. B. Chickov, C. Momma, S. Nolte, F von Alvensleben, A Tünnermann, "Femtosecond, picosecond and nanosecond laser ablation of solids," *Appl. Phys. A* **63**, pp 109-115, 1996.
3. C. Körner, R. Mayerhofer, M. Hartmann, H. Bergmann, " Physical and material aspects in using visible laser pulses of nanosecond duration for ablation," *Appl. Phys. A* **63**, pp 123-131, 1996.

4. A.Luft, U. Franz, A Emsermann, and J. Kaspar " A study of the thermal and mechanical effects on materials induced by pulsed laser drilling," *Appl. Phys. A* **63**, pp 93-101, 1996
5. C. Momma, B. Chickov, S. Nolte, F von Alvensleben, A Tünnermann, H. Welling, B. Wellegehausen, " Short pulse laser ablation of solid targets," *Optics Communications* **129**, pp 134-142, 1996.
6. M. Martynyuk, "Vaporisation and boiling of liquid metal in an exploding wire," *Sov. Phys. Tech . Phys.* **19**, p 793, 1974
7. V. Carey " Liquid-vapor phase-change phenomena: An introduction to the thermophysics of vaporization and condensation processes in heat transfer equipment," *Hemisphere Pub Corp.* pp 1-181, © 1992.
8. R. Kelly and A. Miotello, "Comments on explosive mechanisms of laser sputtering," *Applied Surface Science* **96-98**, pp 205-215, 1996.
9. D. Kapitan, D. Coutts and C. Webb, " On pulsed laser ablation of metals: comparing the relative importance of thermal diffusion in the nanosecond-femtosecond regime," *IEEE Proc. Conf. On Lasers and Electro-Optics Europe* 1998 p 307.
10. A. Mele, A. Giardini Guidoni, R. Kelly, C. Flamini and S. Orlando, " Laser ablation of metals: Analysis of surface heating and plume-expansion experiments," *Applied Surface Science* **109-110**, pp 584-590, 1997
11. R. Mildren, D. Jones and D. Brown, " A 100W, near diffraction limited, copper HyBrID laser oscillator," *J. Phys. D: Appl. Phys.* **31**, pp 1812-1816, 1998.
12. G. Kaye and T. Laby, "Tables of physical and chemical constants," *Longman* 16th Ed, © 1992.
13. M. Martynyuk, " Criticalconstants of metals," *Russian J. Phys. Chem.* **57** (4), pp 494-501, 1983.